Oxygen Transfer between Metals and Oxygen-Ion Conducting Supports

The charge-transfer reactions in the three-phase interfacial region, between a platinum catalyst, an yttria-stabilized zirconia (YSZ) support, and the gas phase, were studied electrochemically during carbon monoxide oxidation. From electrochemical and reaction-rate measurements, it appeared that oxygen was being removed from the support by carbon monoxide adsorbed on the platinum, while being supplied to the support by atomic oxygen adsorbed on either the platinum or the YSZ.

Highly disperse Pt/YSZ catalyst outperformed a Pt/Al_2O_3 catalyst, the rate difference being explained in terms of interfacial reactions. Even in the presence of species such as water and sulfur dioxide, catalysts with YSZ supports outperformed those with alumina supports.

I. S. Metcalfe, S. Sundaresan
Department of Chemical Engineering
Princeton University
Princeton, NJ 08544

Introduction

Supported metals are among the most important industrial catalysts; consequently, much attention has been devoted to understanding their behavior. When an interface exists between support and metal, there may be a transfer of electrons between the metal and support (Herrmann, 1984; Horsely, 1979; Meriaudieau et al., 1982), which may, especially if the metal particles are small, modify the properties of the metal as a catalyst (Akubuiro and Verikios, 1985; Vannice and Garten, 1979). Such phenomena are believed in many cases to be the cause of so-called strong metal-support interactions (SMSI). (It should be pointed out that electron transfer is not the only possible explanation for these observations. Other theories involve the migration of the support onto the metal, blocking certain sites [Raupp and Dumesic, 1985a; Resasco and Haller, 1983; Spencer, 1985], and stabilization of the metal dispersion against sintering [Baker et al., 1979].) Examples of SMSI occur when group VIII metals are deposited on titania (Resasco and Haller, 1983; Tauster et al., 1978; Chen and White, 1983; Disdier et al., 1983), and some other similar semiconductor oxides (Sexton et al., 1982).

SMSI greatly affects chemisorption and catalytic properties in reactions involving species such as hydrogen and carbon monoxide (Chung et al., 1984; Raupp and Dumesic, 1985b, 1986; Tanaka and White, 1983). For example, when titania is used as a support for platinum (as well as other metals such as palladium [Wang et al., 1981], nickel, iridium, and rhodium [Vannice, 1982]) the catalyst exhibits very high activity for the methanation reaction as compared to platinum-on-alumina or -silica catalysts (Vannice et al., 1983). The results of these studies indicate that carbon monoxide adsorption is inhibited in the presence of SMSI, which can lead to higher rates of reaction in cases where carbon monoxide may be responsible for site blockage.

Recently, Burch and Flambard (1982) argued that the support effects observed in their study of the methanation reaction over nickel-on-titania were not due to SMSI as defined in the literature. They proposed that for systems, such as nickel-on-titania, containing large metal particles, support effects would be restricted to the interfacial region, hence the name interfacial metal-support interactions (IMSI). Burch and Flambard postulated that special interfacial sites between the metal and support could be much more active toward carbon monoxide bond breaking.

Although a good deal of attention has been devoted to studying electron transfer between metal and support, it is also conceivable that oxygen transfer between metal and support could occur in the interfacial region, where the metal, support, and gas phase meet (Metcalfe and Sundaresan, 1986). The oxygen ions in the support lattice could migrate to the metal-support interface, in the vicinity of the three-phase region, and from there diffuse onto the metal surface; the reverse process also is possible. In this way the support lattice oxygen could participate in the overall reaction by means of an interfacial reaction.

If it were possible to study a system where oxygen-ion transfer was the only form of charge transfer between the metal and the

Correspondence concerning this paper should be addressed to S. Sundaresan.
The present address of I. S. Metcalfe is Dept. of Chemical Engineering, Imperial College, Prince Consort Road, London SW7, England.

support, then one could measure interfacial transfer rates by electrochemical means. By doing so, one could ascertain whether such interfacial oxygen transfer could influence the overall rate of reaction. Such a catalyst would not exhibit SMSI, as usually defined, since electron transfer to the metal, due to reduction of the support, would be negligible. The catalyst would not be bifunctional, but would exhibit a particular form of IMSI.

When tetravalent oxides (such as zirconia or ceria) are doped with trivalent or divalent oxides (such as yttria or calcia), it is possible to form what is known as an oxygen-ion conducting solid electrolyte (Geller, 1977; Subbarao, 1980). Oxygen-ion conducting solid electrolytes of this type demonstrate mechanisms of oxygen transport similar to those of oxides such as titania or ceria (Blumenthal et al., 1973), while at the same time exhibiting extremely low electronic conductivities. Hence, one would expect a catalyst such as platinum deposited on yttria-stabilized zirconia (Pt/YSZ) to exhibit IMSI but not SMSI. Furthermore, one might expect that the rate of a reaction, like carbon monoxide oxidation, might be greater over such a catalyst, as opposed to a catalyst such as platinum-on-alumina (Pt/Al_2O_3), which would not be expected to exhibit appreciable three-phase reactions. The performances of these two catalysts (Pt/YSZ and Pt/Al_2O_3) were compared at 673 K under various gas-phase conditions; as can be seen in Figure 1, the oxidation rate was always greater over the Pt/YSZ. (The platinum loading was 0.02 wt. %, and the platinum dispersion was very nearly equal for both catalysts; this is discussed in greater detail later. Although the YSZ support also catalyzes the oxidation of carbon monoxide to a small extent, even in the absence of platinum, this rate was found to be an insignificant fraction of the rate reported in Figure 1.) It is quite possible that this difference in carbon monoxide oxidation rates is due to three-phase reaction.

There were four objectives of this research:

1. To develop a technique to measure the three-phase reaction rates for the model system of Pt/YSZ
2. To measure and model the rates of these three-phase reactions under both steady and dynamic conditions
3. To compare the behavior of YSZ as a support to other materials with a view to maximizing catalyst performance

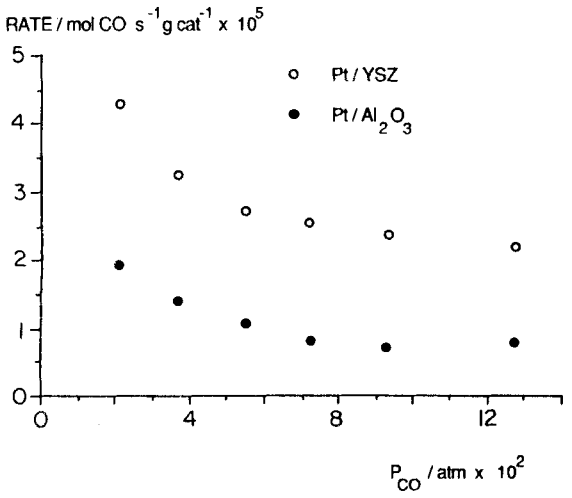

Figure 1. Rate of CO oxidation over Pt/YSZ and Pt/Al_2O_3 catalysts at 673 K.

P_{O_2} = 0.015 atm; platinum loading in each catalyst is 0.02 wt. %

4. To investigate the effect of gas-phase impurities, such as sulfur dioxide, on the rate of the three-phase reactions

As Bockris and Srinivasan (1969) pointed out, it may be possible in a system such as this for equal and opposite, anodic and cathodic, reactions to occur spontaneously at the metal/support/gas-phase interface, exchanging oxygen ions with a common conducting phase (the electrolyte support). Furthermore, for such a system the magnitude of the interfacial reactions should depend directly upon the length of the three-phase contact line, where gas phase, metal, and support are juxtaposed.

To investigate the interfacial reactions, a solid-state electrochemical cell consisting of catalytic platinum electrodes and an YSZ solid electrolyte, was employed. The use of sputtered electrodes with a large crystallite size (approximately 10 μm dia.) enabled a direct electrochemical investigation of the charge transfer (i.e., oxygen transfer) reactions between support and metal under reaction conditions. Surface conditions on the metal were not perturbed because of the extremely low rate of oxygen transfer. In effect, the charge transfer reactions were a high-impedance probe of the metal surface conditions.

Theory

Consider an electrochemical cell made up of two porous platinum electrodes contacting a solid electrolyte, YSZ. Oxygen ions, electrons, and electron holes are all mobile within the oxide. The two electrodes are exposed to two different chemical potentials of oxygen, μ'_{O2} and μ''_{O_2}. The cell may be represented as,

$$\mu'_{O2}, \text{Pt}|\text{YSZ}|\text{Pt}, \mu''_{O_2}$$

For solid electrolytes, the ionic transfer number approaches unity, and the EMF is related to the difference in the chemical potential of oxygen across the cell:

$$E_{cell} = (1/4F)(\mu''_{O_2} - \mu'_{O2})$$

If oxygen at the interfaces is in equilibrium with gas-phase oxygen, there is no chemical reaction, and oxygen behaves as an ideal gas, one obtains the well-known Nernst equation,

$$E_{cell} = (RT/4F) \ln (P''_{O_2}/P'_{O2})$$

Consider a porous platinum electrode deposited on YSZ; the electrode is exposed to a reacting mixture of carbon monoxide and oxygen. The catalytic oxidation of carbon monoxide over platinum can be presented by the following mechanism (Engel and Ertl, 1979):

$$CO(g) + * = CO*; \quad O_2(g) + 2* = 2O*$$
$$CO* + O* \rightarrow CO_2^* + *; \quad CO_2^* = CO_2(g) + *$$

where * denotes a surface site on platinum. The adsorption of CO_2 is considered to be in equilibrium, with the equilibrium being far to the right. It is possible for adsorbed oxygen to participate in charge transfer:

$$O_O + * = O* + V_{\ddot{O}} + 2e' \qquad \text{(R1)}$$

Using the notation of Kroger and Vink (1956), $V_{\ddot{O}}$ denotes an

oxygen-ion vacancy with an effective double positive chage, O_O denotes a lattice oxygen atom, and e' denotes an electron. It is also possible for carbon monoxide to participate in charge transfer reactions in the three-phase region (Kleitz et al., 1976; Okamoto et al., 1980, 1983a, b, 1984a, b):

$$O_O + CO^* = CO_2^* + V_{\ddot{O}} + 2e' \qquad \text{(R2)}$$

Carbon monoxide adsorbed on the platinum strips a lattice oxygen from the electrolyte to form carbon dioxide, leaving an oxygen-ion vacancy in the electrolyte.

The rate of the overall cathodic reaction is given by the sum of the rates of reactions R1c and R2c, the letter c denoting cathodic processes:

$$R_c = l_3(k_{1c}\theta_O + k_{2c}\theta_{CO_2}) \exp(-2\beta F\Delta\phi/RT) \qquad (1)$$

and the rate of the overall anodic reaction is given by the sum of the rates of reactions R1a and R2a, the letter a denoting anodic processes:

$$R_a = l_3(k_{1a}\theta_* + k_{2a}\theta_{CO}) \exp[2(1-\beta)F\Delta\phi/RT] \qquad (2)$$

where subscripts 1 and 2 denote reactions R1 and R2, respectively.

Under open-circuit conditions, anodic and cathodic currents must be equal, their magnitude being related to the equilibrium exchange current density, i_0. Assuming a symmetry factor, β, of one-half:

$$R_c^0 = i_0/2F = l_3 r_{ox} \exp(-F\Delta\phi^0/RT) \qquad (3)$$

$$R_a^0 = i_0/2F = l_3 r_{red} \exp(F\Delta\phi^0/RT) \qquad (4)$$

where

$$r_{ox} = k_{1c}\theta_O + k_{2c}\theta_{CO_2}; \quad r_{red} = k_{1a}\theta_* + k_{2a}\theta_{CO} \qquad (5)$$

It then readily follows that

$$\Delta\phi^0 = (RT/2F) \ln(r_{ox}/r_{red}); \quad i_0 = 2Fl_3(r_{ox}r_{red})^{1/2} \qquad (6)$$

When the double-layer potential at the electrode-electrolyte interface is not equal to its equilibrium value, the interface is said to be polarized. When the interface is polarized, a net current will flow, its magnitude being proportional to the difference between the anodic and cathodic reaction rates: $i = 2F(R_a - R_c)$.

Defining the overpotential η as the difference between the instantaneous double-layer potential and the equilibrium double-layer potential:

$$\eta = \Delta\phi - \Delta\phi^0 \qquad (7)$$

$$i = i_0[\exp(\eta F/RT) - \exp(-\eta F/RT)] \qquad (8)$$

This is a fundamental equation of electrode kinetics and is known as the Butler-Volmer equation.

When $\eta F/RT \ll 1$, it is possible to make a low-field approximation, and the Butler-Volmer equation becomes,

$$i = 2\, i_0 \eta F/RT \qquad (9)$$

and there is a linear relationship between current density and overpotential.

Rearranging Eq. 6, r_{ox} and r_{red} may be expressed in terms of i_0 and $\Delta\phi^0$:

$$r_{ox} = (i_0/2Fl_3) \exp(F\Delta\phi^0/RT) \qquad (10)$$

$$r_{red} = (i_0/2Fl_3) \exp(-F\Delta\phi^0/RT) \qquad (11)$$

Hence, variations in the coverages on the electrode of the oxidizing and the reducing species may be monitored by observing changes in i_0 and $\Delta\phi^0$ at the electrode of interest, designated the working electrode. However, in practice, it is impossible to measure $\Delta\phi^0$. If a counterelectrode is employed, then $E_{wc} = \Delta\phi_w^0 - \Delta\phi_c^0$, where subscripts w and c refer to the working and counterelectrodes, respectively. If the counterelectrode is exposed to invariant conditions, then the potential $\Delta\phi_c^0$ is constant, and changes in $\Delta\phi_w^0$ are reflected in the emf:

$$\Delta\phi_w^0 = E_{wc} + \Delta\phi_c^0 \qquad (12)$$

Substituting Eq. 12 into Eqs. 10 and 11,

$$r_{ox} = (i_0/2Fl_3) \exp(FE_{wc}/RT) \exp(F\Delta\phi_c^0/RT)$$

$$r_{red} = (i_0/2Fl_3) \exp(-FE_{wc}/RT) \exp(-F\Delta\phi_c^0/RT)$$

and defining,

$$R_{ox} = (i_0/2Fl_3) \exp(FE_{wc}/RT) \qquad (13)$$

$$R_{red} = (i_0/2Fl_3) \exp(-FE_{wc}/RT) \qquad (14)$$

R_{ox} and R_{red} can be measured, as described in the next section, and reflect changes in r_{ox} and r_{red}.

In the above analysis, it was assumed that there was no electronic conduction in the support. However, because there is a small degree of electronic conductivity in any solid electrolyte, it is possible for oxygen adsorbed on the solid electrolyte surface to participate in electrochemical reactions. Oxygen atoms adsorbed on the YSZ may migrate into the support (this reaction will be shown to be important later),

$$O_{YSZ}^* + V_{\ddot{O}} \rightarrow {}_{YSZ}^* + O_O + 2h^\bullet \qquad \text{(R3)}$$

forming a lattice oxygen and two electron holes, $h^\bullet$. Such reactions proceed at high enough rates to be responsible for the oxygen semipermeability of YSZ (Fouletier et al, 1976; Kaneko et al., 1987).

Because of the electronic conductivity of the support, the electron holes will migrate to the two-phase region between support and metal, where they will combine with electrons in the metal:

$$e' + h^\bullet \rightarrow \text{null} \qquad \text{(R4)}$$

The rate of reaction R4 is twice that of reaction R3, at steady state, when there is no build up or depletion of electron holes in the support. Hence, the overall cathodic process is,

$$O_{YSZ}^* + V_{\ddot{O}} + 2e' \rightarrow {}_{YSZ}^* + O_O \qquad \text{(R5)}$$

(compare to reaction R1). The rate of the process is determined

by the slower of reactions R3 and R4. (The electron-hole conductivity is only two orders of magnitude lower than the ionic conductivity in YSZ [Fouletier et al., 1976]. Considering that the length of the conduction path for the electron holes is so small [it cannot be much larger than the electrode crystallite dimensions], it seems unlikely that diffusion of electron holes would be rate-limiting [Metcalfe, 1987].)

This cathodic process would be expected to be important under conditions where there is very little adsorbed oxygen present on the metal. Under these conditions, a large potential difference between support and metal exists, and one might expect that the charge-transfer reaction R4, would be fast. Hence, the rate of reaction R3 would be given by,

$$R_{3c} = l_3 k'_{3c} \theta_{O,YSZ} \tag{15}$$

where subscript 3 refers to reaction R3.

Assuming oxygen adsorption-desorption equilibrium on the YSZ (there is very little reaction on the YSZ surface),

$$\theta_{O,YSZ} = K'_2 P_{O_2}^{1/2} / (1 + K'_2 P_{O_2}^{1/2})$$

At the temperatures investigated, one might expect that the coverage of oxygen would be low:

$$\theta_{O,YSZ} = K'_2 P_{O_2}^{1/2}$$

and therefore

$$R_{3c} = l_3 k'_{3c} K'_2 P_{O_2}^{1/2} = l_3 k_{3c} P_{O_2}^{1/2} \tag{16}$$

The rate of the anodic reaction is still given by Eq. 2. The overall rate of the cathodic reaction depends upon the sum of the rates of reactions R1*c* and R3*c*, see Eqs. 1 and 16:

$$R_c = l_3 r_{ox} \exp(-2\beta F \Delta\phi / RT) + l_3 k_{3c} P_{O_2}^{1/2} \tag{17}$$

and expressions for $\Delta\phi^0$ and i_0 can be found. If the contribution of oxygen adsorbed on the YSZ dominates, the rate of the cathodic reaction can be approximated by the rate of reaction R3*c*:

$$R_c = l_3 k_{3c} P_{O_2}^{1/2}$$

and it can be shown that

$$\Delta\phi^0 = (RT/F) \ln (k_{3c} P_{O_2}^{1/2} / r_{red}); \quad i_0 = 2F l_3 k_{3c} P_{O_2}^{1/2} \tag{18}$$

At low overpotentials,

$$i = i_0 \eta F / RT \tag{19}$$

Compare this with Eq. 9.

Experimental Details of Electrochemical System

Electrochemical cell

A solid state electrochemical cell was used to investigate the Pt/YSZ interface:

$$He, CO_2, CO, O_2, Pt | ZrO_2, 8\% Y_2O_3 | Pt, Air$$

The cell itself was in the form of a YSZ thimble, with an internal, painted platinum electrode, and an external, sputtered platinum electrode. From scanning electron microscope (SEM) photographs, the average platinum crystallite size of the external, sputtered electrode appeared to be approximately 10 μm in diameter. The cell was provided in this form by Bendix-Autolite, who manufactured it for use as an automobile exhaust gas sensor.

It was necessary to machine the external electrode to form individual working and reference electrodes. This machining was carried out by Ellis Ceramtek. Two ring electrodes, each 1/8 in. (3.2 mm) wide, were formed. The working and reference electrodes had a projected area of 0.7 and 0.5 cm^2, respectively. The internal counter electrode was left in its original form.

Gold leads were mechanically attached to the two external electrodes. The leads were held in place by a drop by Ceramabond 503 (a very low porosity ceramic bonding agent supplied by Aremco Products, Inc.). A ceramic bridge was formed to prevent the lead from the lower working electrode from coming into contact with the upper reference electrode. Ceramabond 503 was also applied to the leads as an insulator where there was a danger that they might come in contact with the reactor housing.

The thimble was bonded to an alumina disk using the same ceramic bonding agent. The leads from the external electrodes were passed between the alumina disk and the thimble. The lead from the counterelectrode was held in place by a cup and weight arrangement.

The whole thimble and disk assembly was then placed in the aluminum reactor housing, Figure 2. The disk was secured using a stainless steel flange and stainless steel bolts. No O-ring was used in the assembly. On heating, the thermal expansivity mis-

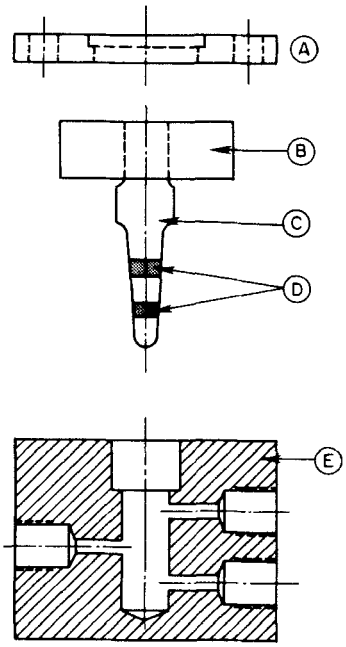

Figure 2. Electrochemical reactor.
A. Retaining flange
B. Ceramic disk
C. YSZ thimble
D. Sputtered platinum electrodes exposed to reaction mixture
E. Aluminum housing

match created a seal, the stress involved being great enough to cause the aluminum to begin to yield and the stainless steel bolts to deform. For these reasons reactors were only used once.

The volume of the empty reaction chamber was 4.0 cm^3; the volume of the thimble portion, which rested inside the reaction chamber, was 1.8 cm^3. Hence, the free gas-phase volume in the reactor was 2.2 cm^3. The reactor had two inlet ports, to aid gas-phase mixing, and one outlet port. The inlet ports were positioned so that the inlet gases would impinge directly on the working and reference electrodes. The inlet and outlet port diameters were 1/8 in. (3.2 mm), to maintain high inlet and outlet gas velocities. Aluminum tubing and fittings were used for all connections that would be heated significantly above room temperature. The whole assembly, housing and thimble, was placed in a box furnace (Sybron-Thermolyne FA 1630), which was fitted with an on/off temperature controller (Omega E 924 K). Typically, the reactor was operated isothermally (Metcalfe, 1987) at 738, 783, and 828 K.

Air at a flow rate of 7.4×10^{-6} mol/s (10 sccm) was passed over the counterelectrode at all times. A net flow rate through the reaction side of 2.2×10^{-4} mol/s (300 sccm) was used (a line regulator was employed to ensure that this flow rate remained constant). A recycle pump (Metal Bellows MB-41) was used to maintain the total flow through the reaction side at about 3.7×10^{-3} mol/s (5,000 sccm) and limit per-pass conversion. This resulted in a space velocity of about 110 s^{-1} at 773 K. The pressure drop experienced across the reactor at these flow rates was about 0.4 atm. Per-pass conversions were typically below 2% under normal operating conditions. Partial pressures of carbon monoxide and oxygen were between 0.005 and 0.05 atm, the balance being helium. The reactor was operated close to atmospheric pressure.

A 1 cm^3 sample loop and gas sampling valve (Supelco six-port switching valve) were fitted to the reactor outlet stream. This allowed a sample of the product gases to be injected into the Gow Mac gas chromatograph (model 69-150). An Alltech CTR-1 column was used to analyze for oxygen, carbon monoxide, and carbon dioxide.

Electrical system

The technique of solid electrolyte potentiometry has recently been used to study oxygen activities at metal electrodes under reaction conditions (Michaels and Vayenas, 1984; Okamoto et al., 1983a, b; Stoukides and Vayenas, 1980; Vayenas and Saltsburg, 1979; Vayenas et al., 1980). However, the use of a three-electrode DC system (Okamoto et al., 1984a, b; Wang and Norwick, 1979a, b; Winnubst et al., 1984) allows the measurement of electrode overpotentials in addition, and is consequently a much more powerful tool. In this study, a three-electrode DC system was employed. This consisted of a counterelectrode, which was exposed to air at all times, and reference and working electrodes, which were exposed to identical reaction conditions. A power supply was used to polarize the working and counterelectrodes, the current being measured by an ammeter.

To determine the exchange current density at the working electrode, a voltage V_{wc} was applied across the working and counterelectrodes. At steady state, a current I flowed in the external circuit. The voltage V_{wc} is related to I in the following way:

$$V_{wc} = E_{wc} + \eta_w(I) + \eta_c(I) + (IR)_{wc}$$

where η_w and η_c are the overpotentials at the working and counterelectrodes (signs being defined relative to the direction of current flow), and $(IR)_{wc}$ is the resistive loss between the working and counterelectrodes. The voltage difference between the unpolarized reference electrode and the polarized counterelectrode, V_{rc}, was also recorded. This voltage V_{rc} is related to I by the equation

$$V_{rc} = E_{rc} + \eta_c(I) + (IR)_{rc}$$

Both signals, V_{wc} and V_{rc}, were sent to an analog multiplexer and oscilloscope, where they were differenced:

$$V_{wc} - V_{rc} = (E_{wc} - E_{rc}) + \eta_w(I)$$

Resistive losses $(IR)_{rc}$ and $(IR)_{wc}$ in the electrolyte itself, which was only about 2 mm thick, were negligible at the temperatures of the investigation (Metcalfe, 1987).

The external power circuit used to polarize the working electrode consisted of an HP 6114 Precision Power Supply in series with a reference resistor and a field-effect transistor (FET) switch, which had the ability to send a digital signal to the oscilloscope for triggering purposes. These three elements were placed across the counter- and working electrodes. The current in the external circuit was measured by monitoring the voltage drop across the reference resistor with a digital multimeter (Simpson model 464). All signals taken from the cell and power circuit were suitably buffered with $10^{12}\ \Omega$ input impedance voltage followers before being displayed.

If the reaction side of the cell behaves as a continuous stirred-tank reactor (CSTR), then $E_{wc} = E_{rc}$ and $V_{wc} - V_{rc} = \eta_w(I)$. The current density, i, is simply equal to the current passed, I, divided by the electrode area. Now, the current-overpotential relationship can be found for the working electrode. Recalling Eq. 9, and rearranging,

$$i_0 = (RT/2F)\left|(di/d\eta)\right|_{\eta \to 0} \tag{20}$$

and the exchange current density can be evaluated from the gradient of the current-overpotential relationship at the origin. However, if the current-overpotential relationship is given by Eq. 19, then

$$i_0 = (RT/F)\left|(di/d\eta)\right|_{\eta \to 0} \tag{21}$$

Electrochemical Results and Discussion

Experiments were performed at three different temperatures, 738, 783, and 828 K, using feed mixtures of carbon monoxide and oxygen in helium. Limited experiments were also undertaken at 673 K to provide data necessary in the analysis of the results from the porous catalysts. The EMF's between each of the reaction-side electrodes and the counter-side electrode, and the exchange current densities of the reaction-side electrodes, were recorded over a range of gas-phase conditions at each of the temperatures. Satisfactory agreement between measurements at the two reaction-side electrodes was demanded, when screening experimental data, to ensure that the reactor behavior was close to that of a CSTR. Figure 3 shows a plot of cell EMF vs. $\log_{10}(P_{CO}/2P_{O_2})$ at each of the three temperatures, gas-phase partial pressures being measured in the reactor outlet stream. Electrochemical cells of the type used in our study are widely

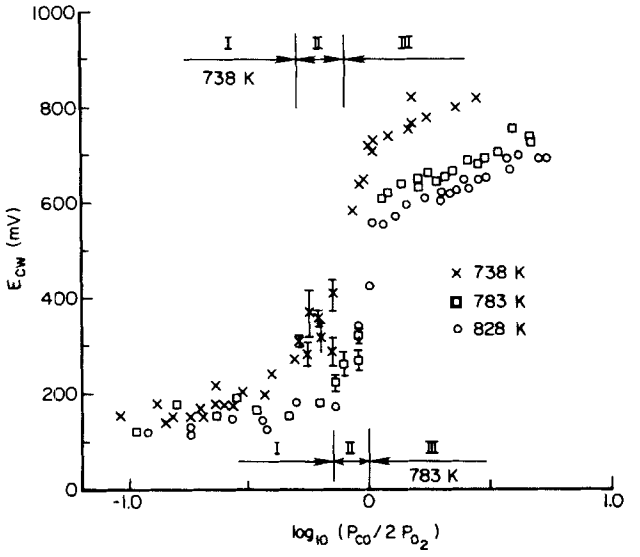

Figure 3. Cell voltage under open-circuit conditions as a function of composition at various temperatures.

used as exhaust-gas oxygen sensors in automobiles. The open-circuit EMF's of such sensors have been studied by a number of researchers, and similar results have been observed (Okamoto et al., 1980, 1983a, b, 1984b).

Three regimes of operation can be identified. Regime I, where the cell EMF is typically below 275 mV, is found at low $P_{CO}/2P_{O_2}$ ratios. At higher ratios, regime III, the cell EMF is typically greater than 600 mV. In regime II, representing the transition from regimes I to III, the cell EMF is very sensitive to the value of $P_{CO}/2P_{O_2}$ indicating adsorbate coverages that are very sensitive to gas phase composition. Self-sustained oscillations in the cell EMF and exchange current density were also observed in this regime. As temperature increases, regime II appears to become narrower and shift towards the stoichiometric point (no oscillations were observed at 828 K, indicating that regime II is very narrow at this temperature). Let us use the variables a and b as estimates of P_{CO}/P_{O_2} when the cell EMF equals 600 and 275 mV, respectively. The values of a and b, Table 1, are used to indicate the bounds of regime II and, as such, should be equal at 828 K.

The purpose of the electrochemical study was to reveal which interfacial reactions are important in the three-phase region and to determine their magnitudes. Exchange current densities and EMF's were used to evaluate R_{ox} and R_{red}, previously described, Eqs. 13 and 14. Reaction rate, R_{ox}, and R_{red} were then correlated with respect to gas-phase composition and temperature. The details of the analysis are described elsewhere (Metcalfe, 1987) and only the salient features of the resulting interpretation are presented below.

Table 1. Limits of Regime II

Temp. K	b P_{CO}/P_{O_2} at 275 mV	a P_{CO}/P_{O_2} at 600 mV
738	1.0	1.6
783	1.5	2.0
828	2.0	2.0

Dependency of rate, exchange current, and EMF on gas-phase conditions

In regime I, it can easily be shown that the rate of carbon monoxide oxidation over platinum is limited by the rate of carbon monoxide adsorption. It was found that oxygen was removed from the YSZ support by the reaction,

$$CO^* + O_O \rightarrow CO_2^* + V_{\ddot{O}} + 2e' \qquad (R2a)$$

and supplied to the support by

$$O^* + V_{\ddot{O}} + 2e' \rightarrow O_O + * \qquad (R1c)$$

Thus, the overall three-phase reaction is

$$CO^* + O^* \rightarrow CO_2^* + *$$

It should be noted that the above reaction can occur, through the Langmuir-Hinshelwood mechanism, anywhere on the Pt crystallite. The interfacial reactions simple provide an additional pathway for this reaction in the three-phase region. As the net effect of the interfacial oxygen transfer process is CO oxidation, the exchange current density is a measure of the rate of carbon monoxide oxidation through the interfacial reactions. However, due to the fact that the rate of reaction is limited by the rate of carbon monoxide adsorption on the platinum, the benefits of interfacial reactions are hardly noticeable in this regime. The focus of our discussion will therefore be on regime III, where three-phase reactions will prove to be quite beneficial. Figure 4 shows plots of carbon monoxide oxidation rate vs. $P_{O_2}/(1 + KP^0_{CO})$, where the quantity P^0_{CO} is defined as,

$$P^0_{CO} = P_{CO} - bP_{O_2} \qquad (22)$$

The quantity K was estimated by demanding an Arrhenius form and using a least-squares method to fit the data at all temperatures, simultaneously. It was found that

$$K = 6.1 \times 10^{-7} \exp(114/RT)\ \text{atm}^{-1} \qquad (23)$$

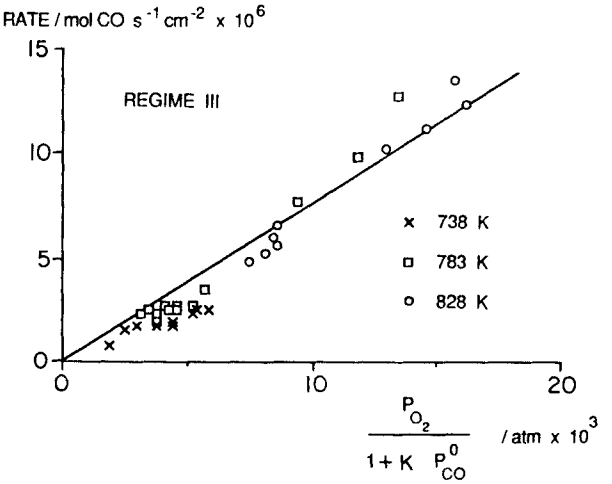

Figure 4. Rate of CO oxidation observed in electrochemical reactor under CO-rich conditions.

The data are consistent with the oxidation rate, being primarily limited by the rate of oxygen adsorption (Engel et al., 1979; Golchet and White, 1978; Herz and Marin, 1980; McCarthy et al., 1975) in this regime. The surface balance for carbon monoxide can be expressed as

$$k'_{a1}P_{CO}\theta_* - \text{Rate} - k_{d1}\theta_{CO} = 0$$

where *Rate* denotes the overall rate of carbon dioxide production. It appears reasonable to assume that the coverage of dissociatively adsorbed oxygen is much lower than the coverage of carbon monoxide molecules, as well as the amount of vacant sites, so that $\theta_* \simeq 1 - \theta_{CO}$.

In this case, the rate of reaction is dependent upon the number of vacant sites available for oxygen adsorption-dissociation, so that we may write

$$\text{Rate} = k'_{a2}P_{O_2}\theta_*$$

where it is assumed that only one vacant site is needed to adsorb an oxygen molecule; k'_{a2} is an effective rate constant for oxygen adsorption coupled with dissociation.

By combining the above equations, it can be shown that the rate of reaction should have the following dependency:

$$\text{Rate} = \frac{k'_{a2}P_{O_2}}{[1 + K_1(P_{CO} - k'_{a2}/k'_{a1}P_{O_2})]} \qquad (24)$$

for $k'_{a1}P_{CO} > k'_{a2}P_{O_2}$, and, for large values of P_{CO}, the usual first-order inhibition by carbon monoxide is observed. In the model, the equilibrium constant for carbon monoxide adsorption-desorption is represented by K_1 and, from a comparison with the functional form obtained from the experimental data analysis, we see that K, eq. 23, is an estimate of K_1.

It has been reasonably well established that at temperatures where self-sustained oscillations in the reaction rate are observed, the processes of adsorption, desorption, and surface reaction exhibit three solutions in the oscillatory regime, the middle solutions always being unstable (Chang and Aluko, 1984; Turner et al., 1981). Furthermore, the oscillations arise as a result of the loss of stability in the other two, otherwise stable, solution branches. These two solution branches, between which oscillations occur, are representative of conditions prevailing in regimes I and III (Burrows et al., 1985; Chang and Aluko, 1984; Turner et al., 1981). Thus, there is ample reason to believe that the solutions in regimes I and III should extend into, and up to the end of, regime II. Therefore, one might expect the value of b, Table 1, to be an estimate of k'_{a2}/k'_{a1}.

From the rate expression, Eq. 24,

$$\theta_* = 1/(1 + K_1P^0_{CO})$$

and as $\theta_* \simeq 1 - \theta_{CO}$,

$$\theta_{CO} = K_1P^0_{CO}/(1 + K_1P^0_{CO})$$

A plot of R_{red} vs. $P^0_{CO}/(1 + KP^0_{CO})$ was found to be linear with zero intercept, Figure 5. This implies that oxygen is primarily removed from the electrolyte by carbon monoxide adsorbed on the platinum:

$$CO^* + O_O \rightarrow CO^*_2 + V_{\ddot{O}} + 2e' \qquad (R2a)$$

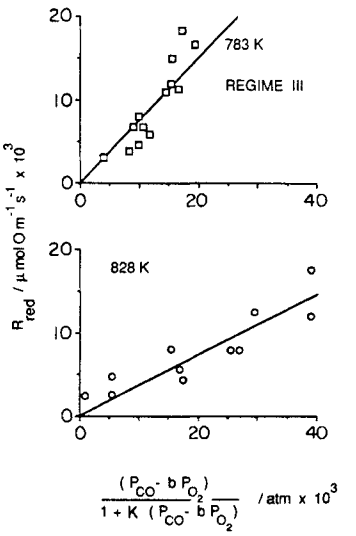

Figure 5. Variation of R_{red}, Eq. 14, as a function of composition under CO-rich conditions.

If the oxidation of the electrolyte occurred by reaction with oxygen adsorbed on the platinum, the square of the exchange current density should be proportional to the rate of carbon monoxide oxidation. This was found not to be the case, because the exchange current density did not decrease as the partial pressure of carbon monoxide was increased. Plots of $i_0/2Fl_3$ vs. $P^{1/2}_{O_2}$ at all three temperatures were also found to be essentially linear, Figure 6, implying that the oxygen must be supplied by oxygen adsorbed on the YSZ:

$$O^*_{YSZ} + V_{\ddot{O}} + 2e' \rightarrow {}^*_{YSZ} + O_O \qquad (R5c)$$

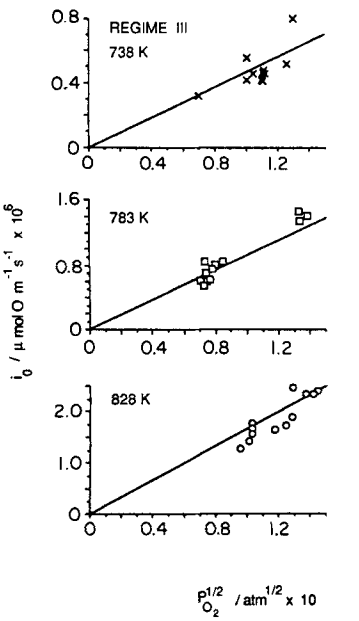

Figure 6. Exchange current density per unit length of three-phase interface in electrochemical reactor under CO-rich conditions.

Discussion of model

The treatment of the experimental data indicated that rate of reaction, i_0, R_{ox}, and R_{red} all depended upon gas-phase conditions in the manners outlined previously. Using the experimental data collected at all three temperatures, preexponential factors and temperature dependencies were found (using a least-squares approach and assuming an Arrhenius form) for the physical rate constants for adsorption, desorption, reaction, etc., in regime III. The details can be found elsewhere (Metcalfe, 1987). We shall present only those results that are relevant for our discussion here.

Using a model with oxygen adsorption on platinum as the rate-determining step for carbon monoxide oxidation in regime III, the fact that exchange current density shows little dependency on the partial pressure of carbon monoxide implies that oxygen atoms adsorbed on the YSZ are transported into the YSZ by reaction R5*c*; the composition dependence of R_{red} implies that oxygen is still removed from the support by reaction R2*a*. From the temperature independence of the gradient of Figure 4, oxygen adsorption appears to be essentially unactivated, which is in reasonable agreement with previous work (Gland et al., 1980). The value for the heat of adsorption of carbon monoxide, implied by K, of 114 kJ/mol is likewise in good agreement with values in the literature (Weinberg and Merrill, 1973). The dominant processes are reactions R2*a* and R5*c*, and the net interfacial reaction is $CO^* + O^*_{YSZ} \rightarrow CO_2(g) + * + {}^*_{YSZ}$. Therefore, the exchange current is a direct measure of interfacial carbon dioxide production. The apparent activation energy for three-phase carbon dioxide production was determined as 71 kJ/mol in regime III,

$$k_{3c} = 4.6 \times 10^{-1} \exp(-71/RT) \mu\text{mol O/m} \cdot \text{s} \cdot \text{atm}^{1/2}$$

If the primary source of oxygen for the reoxidation of the YSZ support was from the platinum crystallites and not the YSZ surface, then the three-phase reactions would have an insignificant effect on the overall rate of carbon monoxide oxidation in this regime (because the rate of carbon monoxide oxidation is already limited by the rate of oxygen adsorption on the platinum). Thus, to increase the rate of reaction, the rate of oxygen arrival to the reaction zone should be increased. The YSZ support introduces another pathway for oxygen to reach the reaction zone. Hence, the support would play a beneficial role if the supply rate of oxygen through the support is comparable to the supply rate through direct adsorption on the platinum.

From experimental values of working electrode exchange current density it is estimated that the rate of interfacial carbon dioxide production is some four orders of magnitude lower than the overall rate of CO oxidation for the 10 μm crytallites in the electrochemical cell; that is, in the electrochemical cell CO oxidation occurs primarily on the platinum surface through the Langmuir-Hinshelwood reaction and the three-phase reactions contribute negligibly to the overall rate of CO oxidation. However, if the platinum crystallite size were reduced by about four orders of magnitude (to approximately 1 nm), one would increase the specific length of the three-phase line by the same factor. Hence, the rate of interfacial carbon dioxide production, being proportional to the length of three-phase contact, should become comparable with the rate of CO oxidation on the Pt surface by the Langmuir-Hinshelwood mechanism. Crystallite sizes of the order of nanometers are quite typical in supported metal catalysts. It appears plausible to expect that a highly disperse Pt/YSZ catalyst should show a significant rate enhancement, caused by three-phase reaction between carbon monoxide adsorbed on the platinum and oxygen adsorbed on the YSZ.

The concept of improving catalytic activity through interfacial processes was further investigated by studying carbon monoxide oxidation over highly disperse, porous, supported metal catalysts.

Porous Supported Catalysts

Reaction rates were investigated over catalysts consisting of platinum dispersed on porous YSZ and alumina supports. Reaction rates were also investigated over platinum deposited on porous titania and ceria supports. Both of these support materials exhibit oxygen-ion conduction and, hence, interfacial oxygen transfer is possible. However, both supports also show substantial electronic conduction and may be expected to show SMSI as well. Thus, under carbon monoxide rich conditions, both Pt/TiO_2 and Pt/CeO_2 should show greater carbon monoxide oxidation rates than Pt/Al_2O_3, because of a combination of both IMSI and SMSI.

Nickel deposited upon the four supports (YSZ, alumina, titania, and ceria) was also investigated. Nickel is a poor catalyst for carbon monoxide oxidation, and any effect due to three-phase reactions may be more pronounced in such a system. For example, although nickel is a poor catalyst for carbon monoxide oxidation, it could be possible for nickel to act as an adsorption site for the carbon monoxide and oxygen, so facilitating interfacial reactions with the support.

Catalyst preparation and experimental details

Highly disperse platinum and nickel catalysts were prepared on four different supports: YSZ, alumina, titania, and ceria (γ-alumina and rutile were used). The supported catalysts were prepared by aqueous impregnation, in the usual way. Supports were first dried and calcined at 773 K for 2 h and then weighed. They were then impregnated with an aqueous solution of platinum or nickel. Solutions of hexachloroplatinic acid (H_2PtCl_6) and nickel nitrate (in nitric acid) were used for impregnation. The metal loading used was approximately 0.02 wt. % in all cases (some higher loadings were prepared to look at catalyst dispersion, as described later). From hydrogen BET adsorption measurements for a 0.1 wt. % Pt/YSZ, it was determined that the platinum dispersion was around 77%. We would conclude that, at the lower loadings of 0.02 wt. % used in these experiments, dispersion should, if anything, be somewhat greater. These dispersions should approach 100%, which is quite usual when employing such a preparation technique at this metal loading (Akubuiro et al., 1985).

The reactors used to investigate the performance of the porous catalyst samples were isobaric, isothermal, tubular, packed-bed, differential reactors. Two reactors were run in parallel, allowing the direct comparison of two catalyst samples (both being held under similar conditions).

The catalyst samples weighed between 0.01 and 1.0 g and were ground to approximately 100 μm dia. and diluted in 10 g of low surface area, 100 μm alumina particles. The catalyst was held in place using plugs of glass wool, which were not catalytically active.

Platinum catalyst results

At 673 K, all four catalysts were compared (i.e., Pt/YSZ, Pt/Al_2O_3, Pt/TiO_2, and Pt/CeO_2), 0.01 g of 0.02 wt. % catalyst being used in each case. The partial pressure of oxygen was held approximately constant, while the partial pressure of carbon monoxide was varied. As expected, in the carbon monoxide rich regime the reaction rate decreased as the partial pressure of carbon monoxide was increased, for all four catalysts, Figure 7.

The Pt/YSZ outperformed the Pt/Al_2O_3 under all conditions investigated. Moreover, the difference in reaction rates between these two catalysts appears to be a weak function of carbon monoxide partial pressure; this can be more clearly seen in Figure 1. If we propose that this difference in reaction rates is due to the presence of three-phase reactions in the Pt/YSZ, then the weak pressure dependency of the rate difference is consistent with the exchange current being a weak function of carbon monoxide partial pressure. It is possible to calculate the length of the three-phase region required in the Pt/YSZ porous catalyst to cause the observed effect.

At the same temperature, under the same gas-phase conditions, results from the electrochemical reactor indicated that the exchange current density was approximately 1.0 $\mu A/cm^2$ at the working electrode. Using the relationship between the rate of interfacial carbon dioxide production and the exchange current density,

$$\text{Interfacial Rate} = i_0/2Fl_3$$

and assuming that charge transfer remains the rate-determining step, gives a value of 1.7×10^{-13} mol CO/m · s converted in the three-phase region for 10 μm dia. crystallites (where $l_3 = 10\pi$ m/cm^2). Now the rate difference between the Pt/YSZ and Pt/Al_2O_3 catalysts is about 1.8×10^{-5} mol CO/s · g cat. Hence, 1.1×10^8 m/g cat of three-phase would be required to cause the observed effect. Using a lattice constant of 0.277 nm for platinum implies a crystallite size of around 1.4 nm dia. (such crystallite sizes are not unusual [Akubuiro et al., 1985]). It is therefore quite possible that three-phase reactions are responsible for the improved performance of the Pt/YSZ over the Pt/Al_2O_3.

The other supports studied, ceria and titania, are both *n*-type semiconductors and show electronic and ionic conduction. Hence, it is possible for ceria and titania to undergo reduction, oxidation, and exhibit SMSI, making any quantitative analysis of the three-phase contribution much more complicated. It is expected that both Pt/TiO_2 and Pt/CeO_2 would show higher rates of carbon dioxide production than Pt/Al_2O_3, because of a combination of three-phase reactions and SMSI. Again this can be seen in Figure 7.

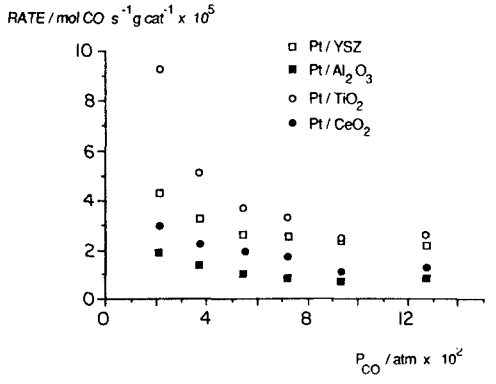

Figure 7. Rate of CO oxidation on a platinum catalyst dispersed over four different supports.

T = 673 K; P_{O_2} = 0.015 atm; platinum loading in each catalyst is 0.02 wt. %

The Pt/TiO_2 seems to be particularly active, outperforming even Pt/YSZ. It is quite possible that interfacial carbon dioxide production is greater in Pt/TiO_2 than in Pt/YSZ. Under the conditions of this experiment, the interfacial rate in the Pt/YSZ catalyst is limited by the capture of oxygen by the support, reaction R5. Because of the greater electronic conductivity of titania, reaction R5 may proceed at higher rates in Pt/TiO_2 than in Pt/YSZ.

From the electrochemical work described earlier, the composition and temperature dependence of the Langmuir-Hinshelwood rate of carbon monoxide oxidation over platinum, in this regime, was found to be of the form,

$$\text{Rate} \propto (P_{O_2}/P^0_{CO}) \exp(-114/RT)$$

Furthermore, using the empirical expression for exchange current density in this regime, the rate of CO oxidation at the three-phase interface is of the form

$$\text{Interfacial Rate} \propto P^{1/2}_{O_2} \exp(-71/RT)$$

One might therefore expect the ratio—the rate of carbon monoxide oxidation by the interfacial reactions divided by the rate of carbon monoxide oxidation by the Langmuir-Hinshelwood reaction on the platinum surface—to decrease as temperature increases. If one accepts the argument that the difference between the rates of CO oxidation over Pt/YSZ and Pt/Al_2O_3 is predominantly due to interfacial CO_2 production, then the relative rate difference, defined as $(Rate_{Pt/YSZ} - Rate_{Pt/Al_2O_3})/Rate_{Pt/Al_2O_3}$, should decrease as temperature increases. A comparision of the experimental results at 673 and 723 K indicated that this indeed was the case (Metcalfe, 1987).

Nickel catalyst results

The motivation for studying nickel catalysts was that nickel, while allowing carbon monoxide and dissociative oxygen adsorption, is a poor catalyst for carbon monoxide oxidation. In theory, it should be possible to take a metal with no activity toward carbon monoxide oxidation and, by depositing the metal on a suitable oxygen-ion conducting support, form an active carbon monoxide oxidation catalyst. The metal would function as an adsorption site, the activity of the catalyst being due solely to interfacial reactions.

The rates of carbon dioxide production over four supported catalysts (Ni/YSZ, Ni/Al_2O_3, Ni/TiO_2, Ni/CeO_2), and the individual supports, were investigated at 673 K, with a constant pressure of oxygen and variable pressure of carbon monoxide, in the same way as for the platinum catalysts. No reaction was detected for the Ni/Al_2O_3 and Ni/CeO_2 systems, or for the individual supports, alumina and ceria (the equipment could detect rates of reaction as low as 3×10^{-8} mol CO/s · g cat at these flow rates and catalyst loadings). Figure 8 shows the rates of reaction over Ni/YSZ and Ni/TiO_2, as well as over the individual supports, YSZ and titania.

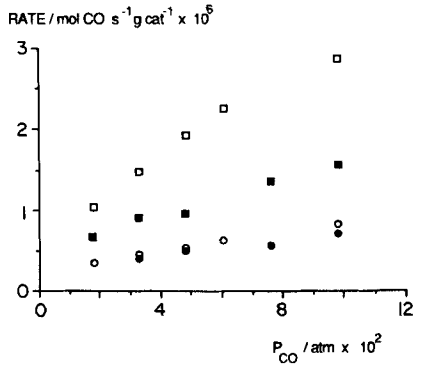

Figure 8. Rate of CO oxidation over various catalyst systems at 673 K.

P_{O_2} = 0.015 atm; O YSZ support only; □ Ni on Ysz at 0.02 wt. % loading; ● TiO_2 support only; ■ Ni on TiO_2 at 0.02 wt. % loading

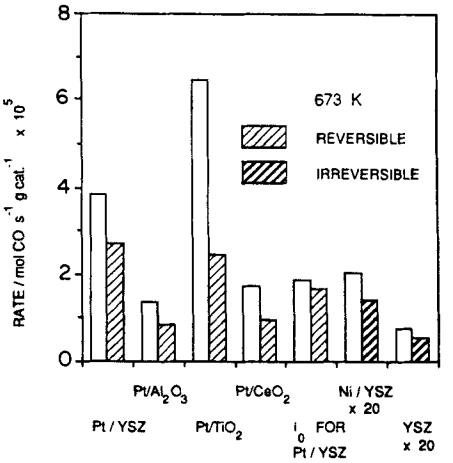

Figure 9. Effect of 20 min exposures to SO_2 on rate of CO oxidation over various catalyst systems.

P_{CO} = 0.03 atm; P_{O_2} = 0.015 atm; P_{SO_2} = 20 ppm

The rates increase with increasing carbon monoxide pressure. If we infer from the Ni/Al_2O_3 result that the rate of carbon monoxide production on the nickel surface is negligible, then the rate difference between the Ni/YSZ and the YSZ must be due to interfacial reactions. It is possible that interfacial reactions also explain the difference between the rates over the Ni/TiO_2 and the titania, although this is not certain, as the difference could be due to SMSI, the nickel being electronically or otherwise modified.

The overall activation energy for the interfacial process in Ni/YSZ is 97 kJ/mol, which is similar to 71 kJ/mol determined electrochemically for Pt/YSZ. The interfacial rate of carbon dioxide production in the Ni/YSZ system appears to be about twenty times lower than that in the Pt/YSZ system. However, Ni/YSZ would still appear to be an attractive, and inexpensive, alternative to a platinum catalyst for carbon monoxide oxidation, because the catalyst loading could quite easily be increased to allow for the lower activity. This is true if a clean environment is provided for the chemical reaction.

Addition of gas-phase impurities

Three-phase reactions may be affected by the presence of species such as water or sulfur dioxide; this would be important in any practical use of a catalyst exhibiting interfacial reactions. Throughout the work presented in this section, the concentrations of inlet carbon monoxide and oxygen were held constant at 0.03 and 0.015 atm, respectively; the temperature of operation was 673 K.

The effect of a 20 ppm level of sulfur dioxide on catalyst performance was investigated, Figure 9. Reaction rates decreased in the presence of sulfur dioxide. The difference in reaction rates over the Pt/YSZ and Pt/Al_2O_3 systems narrowed. This was reflected in a similar decrease in the exchange current density of the Pt/YSZ electrode when exposed to sulfur dioxide. On removing the sulfur dioxide from the inlet streams, the reaction rates over the platinum catalysts, and the exchange current of the Pt/YSZ system, returned to their original values. However, the effect was irreversible in the case of nickel. It appears that sulfur is responsible for a simple site-blocking mechanism on the platinum catalysts and the formation of a stable nickel-sulfur compound with the Ni/YSZ. Sulfur also blocks some of the sites responsible for interfacial reaction in all catalysts.

The effect of 0.025 atm of water added to the inlet gases was also investigated. Water reversibly poisoned the Pt/YSZ and the Ni/YSZ catalysts, but did not poison the other platinum catalysts, Figure 10. (Actually, rates of reaction increased over platinum-on-titania and -ceria supports, possibly due to the occurrence of the water-gas shift reaction.) However, although the difference in rates between the Pt/YSZ and Pt/Al_2O_3 systems was decreased in the presence of water, the exchange current density at the Pt/YSZ electrode actually increased. This suggests that water takes part in interfacial reactions, and, hence, the exchange current is no longer a direct measure of the rate of interfacial carbon dioxide production. It also appears that the presence of water in the interfacial region reduces the number of sites available for interfacial carbon dioxide production. Water may participate in interfacial reactions by an overall process such as the following,

$$H_2O^* + V_{\ddot{O}} + 2e' = 2H^* + O_O \qquad \text{(R6)}$$

Although the response of the nickel catalysts to gas-phase impurities was found to be poor, the dramatic benefits of using

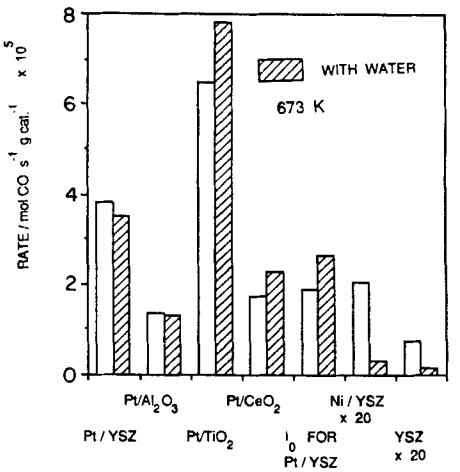

Figure 10. Effect of water vapor on rate of CO oxidation over various catalyst systems.

P_{CO} = 0.03 atm; P_{O_2} = 0.015 atm; P_{H_2O} = 0.025 atm

oxygen-ion conducting supports under clean conditions should not be forgotten. Furthermore, it may be possible to find other metals which, while still much less expensive than noble metals, allow interfacial reactions to proceed, yet are not as susceptible to the presence of impurities.

Other Reaction Systems

Possible relevance to hydrogenation reactions

As mentioned in the Introduction, nickel and platinum, when deposited on titania rather than alumina, show greater activity for the methanation reaction: $CO + 3H_2 = CH_4 + H_2O$. Although this enhancement is often explained in terms of SMSI, interfacial reactions could also be important.

Up to this point, interfacial reactions involving carbon monoxide have all resulted in the removal of oxygen from the support. However, in a strongly reducing atmosphere, such as one of carbon monoxide and hydrogen, it is possible that carbon monoxide would dissociate and donate oxygen to the support:

$$CO^* + V_{\ddot{O}} + 2e' \rightarrow C^* + O_O \qquad (R7)$$

Such a reaction is consistent with the idea of Burch and Flambard (1982) that interfacial sites could be more active for carbon monoxide bond breaking. The occurrence of this reaction also agrees with the results of Gur and Huggins (1981, 1986), who investigated the rates of carbon monoxide and carbon dioxide hydrogenation over a nickel electrode deposited on YSZ (iron, cobalt, and platinum electrodes were also studied). They found that hydrogenation rates were increased when an external voltage of the order of 1 V was applied, in a direction so as to increase the rate of reaction R7. Thus reaction R7, along with the reverse of reaction R6, could be responsible, at least in part, for the observed increase in the methanation activity.

Interfacial reactions could also explain increased reaction rates due to support migration onto the metal surface. When a metal, such as nickel or platinum, is initially deposited on an oxygen-ion conducting support the only three-phase region is that about the metal crystallites. During treatment at elevated temperatures under reducing conditions, the support may be reduced and migrate onto the metal, where it seems to reside in clusters (Ko and Gorte, 1984, 1985). Thus, high-temperature reduction may serve to increase the length of the three-phase region and, hence, the rate of interfacial reaction. Consequently, the overall reaction rate would increase, causing an increase in the observed methanation activity.

Automobile exhaust catalysis

In this publication, we have described the beneficial effects of oxygen-ion conducting supports on the rates of CO oxidation over Pt and Ni catalysts. Such beneficial effects are by no means restricted to Pt and Ni catalysts or to CO oxidation reaction only.

Rh/YSZ catalyst was found to exhibit an appreciably higher rate of CO oxidation than Rh/Al_2O_3 catalyst (Metcalfe, 1987). Currently, rhodium is added to three-way exhaust catalysts to reduce nitric oxide to nitrogen. If nitric oxide adsorbed on rhodium participates in the interfacial oxygen transfer through a reaction such as

$$NO^* + V_{\ddot{O}} + 2e' = N^* + O_O$$

then, according to the reasoning in the present study, the rate of reduction of nitric oxide by carbon monoxide,

$$2NO + 2CO \rightarrow N_2 + 2CO_2$$

over a rhodium catalyst can be enhanced by using an oxygen-ion conducting support instead of an inert support. Indeed, it was fuond that the rate of the above reaction over a Rh/YSZ catalyst was appreciably larger than that over a Rh/Al_2O_3 catalyst (Metcalfe, 1987). The above interpretation ascribing the superior performance of Rh/YSZ catalyst over Rh/Al_2O_3 to the participation of the nitric oxide in the electrochemical reactions is speculative, as there is no direct evidence for such a participation. The only evidence suggesting the possibility of such a participation comes from a study by Pancharatnam et al. (1975), who examined the electrochemical decomposition of NO over a Pt/YSZ system.

It seems that the potential exists to improve the performance of catalysts used for a wide range of reactions involving oxygen transfer, through the use of interfacial reactions.

Summary

Ion transfer in the three-phase region was studied by using a Pt/YSZ electrode exposed to a reacting mixture of carbon monoxide, oxygen, carbon dioxide, and helium. At the temperatures used, 673–828 K, the YSZ support exhibits predominantly ionic conduction, and the cell EMF and electrode exchange current density can be used to determine which anodic and cathodic processes are occurring in the interfacial region. When the catalyst is exposed to carbon monoxide rich conditions, it appears that the dominant cathodic reaction involves oxygen atoms adsorbed on the YSZ surface passing into the bulk of the support and combining with electrons donated from the platinum,

$$O^*_{YSZ} + V_{\ddot{O}} + 2e' \rightarrow O_O + *_{YSZ}$$

The anodic reaction involves the removal of an oxygen ion from the support by reaction with a carbon monoxide molecule adsorbed on the platinum,

$$CO^* + O_O \rightarrow CO_2^* + V_{\ddot{O}} + 2e'$$

Because, under open-circuit conditions, the rates of the anodic and cathodic reactions are equal and opposite, the net reaction in the interfacial region, in the carbon monoxide rich regime of operation, is

$$CO^* + O^*_{YSZ} \rightarrow CO_2(g) + * + *_{YSZ}$$

Therefore, electrode exchange current density is a direct measure of the rate of carbon dioxide production by these interfacial reactions, in both regimes. Under carbon monoxide rich conditions, oxygen adsorption onto the platinum is rate-controlling for large crystallites. So, when an oxygen-ion conducting support is used, it is possible for carbon monoxide adsorbed on the platinum to react with oxygen adsorbed on the YSZ via interfacial reaction. Hence, an extra source of oxygen is present, and one might expect platinum deposited on an oxygen-ion conducting support to outperform platinum deposited on an inert support, under carbon monoxide rich conditions.

As expected, the Pt/YSZ was more active than the Pt/Al_2O_3

for carbon monoxide oxidation, in the carbon monoxide rich regime. Assuming that the enhancement was due to the electrochemical reactions, previously described, would imply a crystallite size of around 1.4 nm. This is a very reasonable value considering the loadings and dispersions of the catalysts.

Both Pt/TiO_2 and Pt/CeO_2 outperformed the Pt/Al_2O_3 for carbon monoxide oxidation, again as expected. In these cases, however, the improved performance may be due to the presence of SMSI (both ceria and titania may easily be reduced, causing electron donation to the platinum) as well as interfacial reactions. The Pt/TiO_2 also outperformed the Pt/YSZ. This could be explained by electronic conduction, which is greater in titania than YSZ, aiding the capture of oxygen from the support surface, and increasing the rate of reaction R5.

Sulfur dioxide poisoned all the catalysts reversibly to about the same degree, as well as reversibly poisoning interfacial reactions. Its presence did not affect the relative activities of the catalysts appreciably.

Water reversibly poisoned three-phase carbon dioxide production, apparently by participating in interfacial reactions at the expense of carbon monoxide. Pt/TiO_2 and Pt/CeO_2 showed higher rates of carbon dioxide production in the presence of water, probably due to the water-gas shift reaction being catalyzed by the supports.

No carbon dioxide production was observed when Ni/Al_2O_3 and Ni/CeO_2 were used. However, both Ni/YSZ and Ni/TiO_2 showed carbon dioxide production, the Ni/YSZ rate being about twice as great as the Ni/TiO_2 rate, but about twenty times lower than the interfacial rate of carbon dioxide production over the Pt/YSZ. Nevertheless, it is possible to create an active catalyst relying upon interfacial reactions by using an otherwise inactive metal with a suitable support.

The effect of sulfur dioxide on the performance of the nickel catalysts was different from its effect on the platinum catalysts in an important way. Sulfur dioxide poisoned the nickel catalysts irreversibly, so rendering nickel useless as a carbon monoxide oxidation catalyst wherever appreciable sulfur dioxide is present. Water poisoned the nickel catalysts reversibly, in the same way as the platinum catalysts were poisoned. However, it is quite possible that another relatively cheap metal, when used with a suitable support, could show a significant activity toward carbon monoxide oxidation, while being less susceptible to the effects of sulfur dioxide and water.

In conclusion, when ionic conductivity is present in a catalyst support, interfacial reactions can play an important role in influencing the overall behavior of the catalyst. These interfacial reactions can explain the enhanced rate of carbon monoxide oxidation over Pt/YSZ compared to Pt/Al_2O_3, as well as the improved performance of Ni/YSZ over Ni/Al_2O_3, and Rh/YSZ over Rh/Al_2O_3. *Other reactions, such as the carbon monoxide-nitric oxide reaction,* can also show higher rates when an oxygen-ion conducting support is used.

Furthermore, our work has shown that when oxygen-ion conductors are used as supports, results should not be explained in terms of strong metal-support interactions alone. The influence of reactions in the interfacial region must also be considered.

Finally, an ideal application of YSZ would appear to be as a support in automobile exhaust treatment catalysts. Both platinum and rhodium, the two main constituents of automobile exhaust treatment catalysts, exhibit improved performance when deposited on YSZ rather than alumina. This is true over a wide range of temperatures and compositions, representative of automobile exhaust, and even in the presence of species such as sulfur dioxide and water.

Acknowledgment

This work was supported by the National Science Foundation, Grant No. CPE-8307199, and the Shell Foundation. We are grateful to the Bendix-Autolite Company for providing the zirconia thimbles.

Notation

a, b = bounds of regime II, Table 1
E, E_{cell} = EMF, V
E_{rc} = EMF between reference and counterelectrodes, V
E_{wc} = EMF between working and counterelectrodes, V
F = Faraday constant, 9.654×10^4 C/mol
i = current density, A/cm^2
i_0 = exchange current density, A/cm^2
I = current, A
$(IR)_{rc}$ = resistive potential drop between reference and counterelectrodes, V
$(IR)_{wc}$ = resistive potential drop between working and counterelectrodes, V
k_{1a} = anodic rate constant for reaction R1, mol O/m · s
k_{1c} = cathodic rate constant for reaction R1, mol O/m · s
k_{2a} = anodic rate constant for reaction R2, mol O/m · s
k_{2c} = cathodic rate constant for reaction R2, mol O/m · s
k_{3c} = modified cathodic rate constant for reaction R3, Eq. 16, mol O/m · s · atm$^{1/2}$
k'_{3c} = cathodic rate constant for reaction R3, mol O/m · s
k'_{a1} = rate constant for CO adsorption in regime III, mol CO/atm · s · cm^2
k'_{a2} = rate constant for oxygen adsorption in regime III, mol O/atm · s · cm^2
k_{d1} = rate constant for CO desorption, mol CO/s · cm^2
K = experimental estimate of K_1, atm^{-1}
K_1 = equilibrium constant for CO adsorption, atm^{-1}
K'_2 = equilibrium constant for atomic oxygen adsorption on YSZ, atm$^{-1/2}$
l_3 = specific length of three-phase contact, m/cm^2
P_{CO} = partial pressure of carbon monoxide, atm
P^0_{CO} = excess partial pressure of carbon monoxide in regime III, Eq. 22, atm
P_{O_2} = partial pressure of oxygen, atm
r_{ox}, r_{red} = quantities, Eq. 5, mol O/m · s
R = gas constant, 8.314 J/mol · K
R_a, R_c = rates of anodic and cathodic reactions, mol/s · cm^2
R^0_a, R^0_c = equilibrium rates of anodic and cathodic reactions, mol/s · cm^2
R_{ox}, R_{red} = quantities, Eqs. 13, 14, mol O/m · s
Rate = rate of CO_2 production, mol CO_2/s · cm^2
T = temperature, K
V_{wc}, etc. = potential difference between respective electrodes, V

Greek letters

β = symmetry factor
η = overpotential, V
η_w, η_c = overpotential at working and counterelectrodes, V
θ_{CO} = coverage of carbon monoxide
θ_{CO_2} = coverage of carbon dioxide
θ_O = coverage of atomic oxygen
θ_* = fraction of vacant sites
$\theta_{O,YSZ}$ = coverage of atomic oxygen on YSZ
$\theta_{*,YSZ}$ = fraction of vacant sites on YSZ
μ_i = chemical potential of species i, J/mol
ϕ = electrical potential, V
$\Delta\phi$ = potential difference at electrode-electrolyte interface, V
$\Delta\phi^0$ = equilibrium potential difference, V
$\Delta\phi_w$ = potential difference at working electrode, V
$\Delta\phi_c$ = potential difference at counter electrode, V
$\Delta\phi^0_w$ = equilibrium potential difference at working electrode, V
$\Delta\phi^0_c$ = equilibrium potential difference at counterelectrode, V

Literature Cited

Akubuiro, E. C., and X. E. Verykios, "Dispersion and Support Effects in Carbon Monoxide Oxidation over Platinum," *Appl. Catal.*, **14,** 215 (1985).

Baker, R. T., E. B. Prestridge, and R. L. Garten, "Electron Microscopy of Supported Metal Particles. II: Further Studies of Platinum/Titania," *J. Catal.*, **56,** 390 (1979).

Blumenthal, R. N., F. S. Brugner, and J. E. Garnier, "The Electrical Conductivity of Calcia-Doped Nonstoichiometric Cerium Dioxide from 700 to 1,500 Celsius," J. Electrochem. Soc., **120,** 1230 (1973).

Bockris, J. O'M., and S. Srinivasan, *Fuel Cells and Their Electrochemistry,* McGraw-Hill, New York, vi (1969).

Burch, R., and A. R. Flambard, "Strong Metal-Support Interactions in Nickel/Titania Catalysts: The Importance of Interfacial Phenomena," *J. Catal.*, **78,** 389 (1982).

Burrows, V. A., S. Sundaresan, Y. J. Chabal, and S. B. Christman, "Studies on Self-Sustained Reaction-Rate Oscillations. I: Real-Time Surface Infrared Measurements During Oscillatory Oxidation of Carbon Monoxide on Platinum," *Surf. Sci.*, **122,** 160 (1985).

Chang, H. C., and M. Aluko, "Multiscale Analysis of Exotic Dynamics in Surface Catalyzed Reactions. I: Justification and Preliminary Model Discriminations," *Chem. Eng. Sci.*, **39,** 37 (1984).

Chen, B.-H., and J. M. White, "Properties of Platinum Supported on Oxides of Titanium," *J. Phys. Chem.*, **87,** 1327 (1983).

Chung, Y.-W., G. M. Xiong, and C.-C. Kao, "Mechanism of Strong Metal-Support Interaction in Nickel/Titania," *J. Catal.*, **85,** 237 (1984).

Disdier, J., J.-M. Herrmann, and P. Pichat, "Platinum/Titanium Dioxide Catalysts. A Photoconductivity Study of Electron Transfer from the Ultraviolet-Illuminated Support to the Metal and of the Influence of Hydrogen," *J. Chem. Soc. Faraday Trans. I,* **79,** 651 (1983).

Engel, T., and G. Ertl, "Elementary Steps in the Catalytic Oxidation of Carbon Monoxide on Platinum Metals," *Adv. Catal.*, **28,** 2 (1979).

Fouletier, J., P. Fabry, and M. Kleitz, "Electrochemical Semipermeability and the Electrode Microsystem in Solid Oxide Electrolyte Cells," *J. Electrochem. Soc.*, **133,** 204 (1976).

Geller, S., ed., *Solid Electrolytes,* Springer-Verlag, Berlin-Heidelberg (1977).

Gland, J. L., B. A. Sexton, and G. B. Fisher, "Oxygen Interactions with the Platinum(111) Surface," *Surf. Sci.*, **95,** 587 (1980).

Golchet, A., and J. M. White, "Rates and Coverages in the Low-Pressure Platinum-Catalyzed Oxidation of Carbon Monoxide," *J. Catal.*, **53,** 266 (1978).

Gur, T. M., and R. A. Huggins, "Electrocatalytic Synthesis of Methane on Stabilized Zirconia from Hydrogen/Carbon Dioxide Mixtures," *Solid State Ionics,* **5,** 563 (1981).

———, "Methane Synthesis over Transition Metal Electrodes in a Solid State Ionic Cell," *J. Catal.*, **102,** 443 (1986).

Herrmann, J.-M., "Electronic Effects in Strong Metal-Support Interactions between Platinum and Titanium Dioxide," *J. Catal.*, **89,** 404 (1984).

Herz, R. K., and S. P. Marin, "Surface Chemistry Models of Carbon Monoxide Oxidation on Supported Platinum Catalysts," *J. Catal.*, **65,** 281 (1980).

Horsely, J. A., "A Molecular Orbital Study of Strong Metal-Support Interaction between Platinum and Titanium Dioxide," *J. Am. Chem. Soc.*, **101,** 2870 (1979).

Kaneko, H., W. C. Maskell, and B. C. H. Steele, "Miniature Oxygen Pump-Gauge. I: Leakage Considerations," *Solid State Ionics,* **22,** 161 (1987).

Kleitz, M., P. Fabry, and E. Schouler, *Electrode Processes in Solid State Ionics,* M. Kleitz, J. Dupuy, eds., Reidel, Dordrecht (1976).

Ko, C. S., and R. J. Gorte, "Evidence for Diffusion of a Partially Oxidized Titanium Species into Bulk Platinum," *J. Catal.*, **90,** 59 (1984).

———, "Characterization of Oxide Impurities on Platinum and Their Effect on the Adsorption of Carbon Monoxide and Hydrogen," *Surf. Sci.*, **155,** 296 (1985).

Kroger, F. A., and H. J. Vink, *Solid State Physics,* v. 3, F. Seitz, D. Turnbull, eds., Academic Press, New York, 307 (1956).

McCarthy, E., J. Zahradnik, G. C. Kuczynski, and J. J. Carberry, "Some Unique Aspects of Carbon Monoxide Oxidation on Platinum," *J. Catal.*, **39,** 29 (1975).

Meriaudieau, P., O. E. Ellestad, M. Dufaux, and C. Naccache, "Metal-Support Interaction. Catalytic Properties of Titania-Supported Platinum, Iridium, and Rhodium," *J. Catal.*, **75,** 243 (1982).

Metcalfe, I. S., "Interfacial Oxygen Transfer between Metals and Oxygen-Ion Conducting Supports," Ph.D. Thesis, Princeton Univ., Princeton, NJ (1987).

Metcalfe, I. S., and S. Sundaresan, "Oxygen Storage in Automobile Exhaust Catalysis," *Chem. Eng. Sci.*, **41,** 1109 (1986).

Michaels, J. N., and C. G. Vayenas, "Kinetics of Vapor-Phase Electrochemical Oxidative Dehydrogenation of Ehtylbenzene," *J. Catal.*, **85,** 477 (1984).

Okamoto, H., H. Obayashi, and T. Kudo, "Carbon Monoxide Gas Sensor Made of Stabilized Zirconia," *Solid State Ionics,* **1,** 319 (1980).

Okamoto, H., G. Kawamura, and T. Kudo, "Interpretation of the Electromotive Forces of Solid Electrolyte Concentration Cells During Carbon Monoxide Oxidation on Platinum," *J. Catal.*, **82,** 322 (1983a).

———, "Electromotive Force Studies of Carbon Monoxide Oxidation on Platinum," *J. Catal.*, **82,** 332 (1983b).

———, "Relation between Surface Adsorption States and EMF in a Solid Electrolyte Concentration Cell During Carbon Monoxide Oxidation on Platinum Studied by Local Current Measurement," *J. Catal.*, **86,** 437 (1984a).

———, "Carbon Monoxide Oxidation on Platinum Studied by Local Current and EMF in a Solid Electrolyte Concentration Cell," *J. Catal.*, **87,** 1 (1984b).

Pancharatnam, S., R. A. Huggins, and D. M. Mason, "Catalytic Decomposition of Nitric Oxide on Zirconia by Electrolytic Removal of Oxygen," *J. Electrochem. Soc.*, **122,** 869 (1975).

Raupp, G. B., and J. A. Dumesic, "Effect of Varying Titania Surface Coverage on the Chemisorptive Behavior of Nickel," *J. Catal.*, **95,** 587 (1985a).

———, "Effects of Titania on the Coadsorption of Hydrogen and Carbon Monoxide on Nickel Surfaces: Consequences for Understanding Methanation over Titania-Supported Nickel Catalysts," *J. Catal.*, **96,** 597 (1985b).

———, "Effect of Titanium Oxidation State on the Chemisorptive Properties of Titania-Supported Nickel," *J. Catal.*, **97,** 85 (1986).

Resasco, D. E., and G. L. Haller, "A Model of Metal-Oxide Support Interaction for Rhodium on Titania," *J. Catal.*, **82,** 279 (1983).

Sexton, B. A., A. E. Hughes, and K. Foger, "XPS Investigation of Strong Metal-Support Interactions on Group IIIa-Va Oxides," *J. Catal.*, **77,** 85 (1982).

Spencer, M. S., "Models of Strong Metal-Support Interaction (SMSI) in Platinum on Titania Catalysts," *J. Catal.*, **93,** 216 (1985).

Stoukides, M., and C. G. Vayenas, "Solid Electrolyte Aided Study of the Ethylene Oxidation on Silver," *J. Catal.*, **64,** 18 (1980).

Subbarao, E. C., ed., *Solid Electrolytes and Their Applications,* Plenum, New York (1980).

Tanaka, K., and J. M. White, "Infrared Studies of Carbon Monoxide Adsorption on Reduced and Oxidized Platinum/Titania," *J. Catal.*, **79,** 81 (1983).

Tauster, S. J., S. C. Fung, and R. L. Garten, "Strong Metal-Support Interactions. Group VIII Noble Metals Supported on Titania," *J. Am. Chem. Soc.*, **100,** 170 (1978).

Turner, J. E., B. C. Sales, and M. B. Maple, "Oscillatory Oxidation of Carbon Monoxide over a Platinum Catalyst," *Surf. Sci.*, **103,** 54 (1981).

Vannice, M. A., "Titania-Supported Metals as Carbon Monoxide Hydrogenation Catalysts," *J. Catal.*, **74,** 199 (1982).

Vannice, M. A., and R. L. Garten, "Metal-Support Effects on the Activity and Selectivity of Nickel Catalysts in Carbon Monoxide/Hydrogen Synthesis Reactions," *J. Catal.*, **56,** 236 (1979).

Vannice, M. A., C. C. Twu, and S. H. Moon, "SMSI Effects on Carbon Monoxide Adsorption and Hydrogenation on Platinum Catalysts. I: Infrared Spectra of Adsorbed Carbon Monoxide Prior to and During Reaction Conditions," *J. Catal.*, **79,** 70 (1983).

Vayenas, C. G., and H. Saltsburg, "Chemistry at Catalytic Surfaces: The Sulfur Dioxide Oxidation on Noble Metals," *J. Catal.*, **57,** 296 (1979).

Vayenas, C. G., B. Lee, and J. N. Michaels, "Kinetics, Limit Cycles, and Mechanism of the Ethylene Oxidation on Platinum," *J. Catal.*, **66,** 36 (1980).

Wang, D. Y., and A. S. Nowick, "Cathodic and Anodic Polarization

Phenomena at Platinum Electrodes with Doped Ceria as Electrolyte. I: Steady State Overpotential," *J. Electrochem. Soc.*, **126,** 1155 (1979a).
———, "Cathodic and Anodic Polarization Phenomena at Platinum Electrodes with Doped Ceria as Electrolyte. II: Transient Overpotential and AC Impedance," *J. Electrochem. Soc.*, **126,** 1166 (1979b).
———, "Polarization Phenomena Associated with Reduction of a Doped Ceria Electrolyte," *J. Electrochem. Soc.*, **127,** 113 (1979c).
Wang, S.-Y., S. H. Moon, and M. A. Vannice, "The Effect of SMSI (Strong Metal-Support Interaction) Behavior on Carbon Monoxide Adsorption and Hydrogenation on Palladium Catalysts. II: Kinetic Behavior of the Methanation Reaction," *J. Catal.*, **71,** 167 (1981).
Weinberg, W. H., and R. P. Merrill, "Crystal Field Surface Orbital-Bond-Energy Bond-Order (CFSO-BEBO) Model for Chemisorption. Application to Hydrogen Adsorption on a Platinum(111) Surface," *Surf. Sci.*, **39,** 206 (1973).
Winnubst, A. J., A. H. A. Scharenborg, and A. J. Burggraaf, "The Electrode Resistance of Zirconia-Yttria (-Bismuth[III] Oxide) Solid Electrolytes with Platinum Electrodes," *Solid State Ionics*, **14,** 319 (1984).

Manuscript received May 15, 1987, and revision received Aug. 3, 1987.